Study of the Two-Dimensional $[MM'(C_3H_2O_4)_2(H_2O)_4]$ (M = Ba, Sr and M′ = Cu, Mn) Systems: Synthesis, Structure, Magnetic Properties, and Thermal Decomposition

I. Gil de Muro,[†] F. A. Mautner,[‡] M. Insausti,[†] L. Lezama,[†] M. I. Arriortua,[§] and T. Rojo*[,†]

Departamentos de Química Inorgánica y Mineralogía-Petrología, Facultad de Ciencias, Universidad del País Vasco, Apdo. 644, E-48080 Bilbao, Spain and Institut für Physikalische und Theoretische Chemie, Technische Universität Graz, Rechbauerstrasse 12, A-8010 GRAZ, Austria

Received January 6, 1998

Compounds with the general formula $[MM'(C_3H_2O_4)_2(H_2O)_4]$ (M = Ba, Sr; M′ = Cu, Mn; $C_3H_2O_4$ = malonate) have been synthesized and characterized. Single-crystal X-ray diffraction study on the $[SrCu(C_3H_2O_4)_2(H_2O)_4]$ compound indicates that it crystallizes in the orthorhombic space group, *Pccn*, $Z = 4$, with unit cell parameters $a = 6.719(2)$, $b = 18.513(7)$, and $c = 9.266(4)$ Å. The structure consists of distorted octahedral copper(II) species which are extended along the *ac* plane forming a two-dimensional structure. The geometry of the alkaline-earth ions resembles a distorted antiprism. The other compounds are isostructural. The EPR spectra of the $[MCu(C_3H_2O_4)_2(H_2O)_4]$ (M = Ba, Sr) compounds show an orthorhombic **g** tensor as consequence of a linear combination of the axial symmetry and the exchange interactions between magnetically different centers, but crystallographically equivalent. For the manganese compounds, the EPR spectra of polycrystalline samples show that the intensity of the signal increases with decreasing temperature down to 20 K, and at lower temperatures the intensity decreases, becoming silent below 7 K. Magnetic measurements show two-dimensional (2D) ferromagnetic and antiferromagnetic interactions for the copper and manganese phases, respectively. In all cases, the susceptibility data were fitted by the expression for a Heisenberg square-planar system. The obtained *J/k* values are 1.44 and 1.15 K, for the SrCu and BaCu compounds, respectively, and −0.65 and −0.59 K for the SrMn and BaMn compounds, respectively. For the manganese compounds, magnetic measurements show a magnetic ordering below 5 K which confirms the presence of a weak ferromagnetism. Thermal analyses of the phases show three different decomposition steps: dehydration, ligand pyrolysis, and evolution of the inorganic residue for all compounds. Taking these results into account, we performed further thermal treatments to obtain mixed oxides. These were obtained at short reaction times and at temperatures lower than those of the conventional ceramic method.

Introduction

In the past few years, mixed oxides with transition metals have been widely investigated because of their electrical and magnetic properties, in areas such as superconductivity or magnetoresistance.[1−3] Traditionally, the ceramic method has been employed to get mixed oxides. Nevertheless, and in some cases, thermal decomposition of heterometallic complexes has been discovered to be a more advantageous way.[4,5] In this sense, different compounds containing edta, oxalate, tartrate, and malonate as ligands have been synthesized and used as precursors.[6,7] As a result, the oxides obtained from these precursors were formed at heating times that were shorter and temperatures that were lower than those of other methods. In addition, the use of soft chemical routes can yield homogeneous phases with small grain size.[8]

The chemistry of heteronuclear complexes involving carboxylate-bridged ligands has been investigated exhaustively aided by a wide variety of physical techniques such as electronic spectroscopy, susceptibility measurements, and EPR spectroscopy.[4,9] The malonate ligand, in the bischelating coordination mode, has been shown to be a useful tool for connecting different metals and transmitting different magnetic interactions. In this way, ferromagnetically[10] or antiferromagnetically[11] coupled dimers and alternating chains[12] have been obtained. As

* To whom correspondence should be addressed. E-mail: qiproapt@lg.ehu.es. FAX: 34-4-4648500.
† Departamento de Química Inorgánica.
‡ Departamento de Mineralogía−Petrología.
§ Institut für Physikalische und Theoretische Chemie.

(1) (a) Müller-Buschbaum, H. *Ang. Chem. Ed., Int. Engl.* **1991**, *30*, 723. (b) Sundar Manoharan, S.; Patil, K. C. *J. Solid State Chem.* **1993**, *102*, 267.
(2) (a) von Helmot, R.; Weckes, J.; Holzapfel, B.; Schultz, L.; Samwer, K. *Phys. Rev. Lett.* **1993**, *71*, 2331. (b) McCormack, M.; Jin, S.; Tiefel, T. H.; Fleming, R. M.; Phillips, J. M. *Appl. Phys. Lett.* **1994**, *64*, 3045.
(3) Rao, C. N. R.; Cheetham, A. K.; Mahesh, R. *Chem. Mater.* **1996**, *8*, 2421.
(4) (a) Insausti, M.; Cortés, R.; Arriortua, M. I.; Rojo, T.; Bocanegra, E. H. *Solid State Ionics* **1993**, *63*−*65*, 351. (b) Insausti, M.; Pizarro, J. L.; Lezama, L.; Cortés, R.; Bocanegra, E. H.; Arriortua, M. I.; Rojo, T. *Chem. Mater.* **1994**, *6*, 707.
(5) Rhine, W. E.; Hallock, R. B.; Davis, W. M.; Wong-Ng, W. *Chem. Mater.* **1992**, *4*, 1208.
(6) García-Jaca, J.; Larramendi, J. I. R.; Insausti, M.; Arriortua, M. I.; Rojo, T. *J. Mater. Chem.* **1995**, *5*, 1995.
(7) Insausti, M.; Gil de Muro, I.; Lorente, L.; Rojo, T.; Bocanegra, E. H.; Arriortua, M. I. *Thermochim. Acta* **1996**, *287*, 81.
(8) Beltrán-Porter, D.; Martínez-Tamayo, E.; Ibáñez, R.; Beltrán-Porter, A.; Folgado, J. V.; Escrivá, E.; Muñoz, V.; Segura, A.; Cantanero, A. *Solid State Ionics* **1989**, *32*−*33CP*, 1160.
(9) Clegg, W. *Acta Crystallogr.* **1989**, *147*, 353.
(10) Scaringe, R. P.; Hatfield, W. E.; Hodgson, D. J. *Inorg. Chem.* **1977**, *16*, 1600.
(11) Chattopadhyay, D.; Chattopadhyay, S. K.; Lowe, P. R.; Schwalke, C. H.; Mazumber, S. K.; Rana, A.; Ghosh, S. *J. Chem. Soc., Dalton Trans.* **1993**, 913.
(12) Saadeh, S. H.; Trojan, K. L.; Kampf, J. W.; Hatfield, W. E.; Peroraro, V. L. *Inorg. Chem.* **1993**, *32*, 3034.

S0020-1669(98)00013-5 CCC: $15.00
Published on Web 06/13/1998

far as we are aware, no examples of two-dimensional systems with malonate as ligand have been reported in the literature.

Taking into account the ability of the malonate ligand to form binuclear complexes that can be used as precursors of mixed oxides, we isolated and structurally characterized four new two-dimensional (2D) compounds $[SrCu(C_3H_2O_4)_2(H_2O)_4]$, $[BaCu(C_3H_2O_4)_2(H_2O)_4]$, $[SrMn(C_3H_2O_4)_2(H_2O)_4]$, and $[BaMn(C_3H_2O_4)_2(H_2O)_4]$, which will hereafter be abbreviated as SrCu, BaCu, SrMn, and BaMn, respectively. Magnetic measurements for the copper compounds indicate the presence of ferromagnetic coupling between the copper(II) ions, while antiferromagnetic interactions have been observed in the manganese(II) compounds.

Experimental Section

Materials. Manganese(II) nitrate, copper(II) chloride, barium chloride, sodium carbonate, and malonic acid were purchased from Aldrich Co., while strontium chloride was purchased from Merck. All of them were used without further purification.

Synthesis of Compounds. The compounds were prepared in the following way. A water solution of malonic acid was neutralized with sodium carbonate, after which the salt of the transition metal was added. The solutions were stirred without heating for about 1 h, and then they were mixed with the corresponding alkaline-earth chloride solution in a diffusion device. After 2 days, rhombohedral pale-blue crystals were collected for the copper compounds, and colorless planar prisms were obtained for the manganese compounds. The crystals were washed with water and acetone and dried over P_2O_5. Good quality, single crystals were obtained only for the SrCu compound. Attempts to obtain single crystals for the other compounds have been unsuccessful.

The results of the elemental analysis were consistent with the following stoichiometries: Calc for $C_6H_{12}O_{12}SrCu$: C, 16.87; H, 2.83; Sr, 20.51; Cu, 14.87. Found: C, 16.97; H, 2.64; Sr, 20.86; Cu, 14.65. Calc for $C_6H_{12}O_{12}BaCu$: C, 15.11; H, 2.43; Ba, 28.79; Cu, 13.32. Found: C, 15.13; H, 2.53; Ba, 29.28; Cu, 12.92. Calc for $C_6H_{12}O_{12}SrMn$: C, 17.20; H, 2.86; Sr, 20.93; Mn, 13.12. Found: C, 16.95; H, 2.81; Sr, 20.42; Mn, 12.50. Calc for $C_6H_{12}O_{12}BaMn$: C, 15.38; H, 2.58; Ba, 29.32; Mn, 11.73. Found: C, 14.95; H, 2.11; Ba, 28.31; Mn, 11.49.

Physical Measurements. Microanalyses were performed with a Perkin-Elmer 2400 CHN analyzer. Analytical measurements were carried out in an ARL 3410+ICP with Minitorch equipment. IR spectra ($400-4000$ cm^{-1}) were recorded on a Mattson FTIR 1000 spectrophotometer with samples prepared as KBr pellets. The powder X-ray diffraction (XRD) pattern was taken using a Philips X'pert diffractometer equipped with graphite-monochromated Cu Kα_1 radiation. Data were collected by scanning in the range $5° < 2\theta < 70°$ with increments of $0.02°(2\theta)$. Magnetic susceptibilities of powdered samples were carried out in the temperature range $1.8-300$ K using a Quantum Design MPMS-7 Squid magnetometer. The magnetic measurements were performed at magnetic fields between 0 and 7 T. Electron paramagnetic resonance (EPR) spectra were recorded on a Bruker ESP300 spectrometer, equipped with a standard Oxford low-temperature device operating at X- and Q-bands. The magnetic field was measured with a Bruker BNM 200 gaussmeter, and the frequency was determined by using a Hewlett-Packard 5352B microwave frequency counter. Thermogravimetric measurements were performed in a Perkin-Elmer system-7 DSC-TGA instrument. Crucibles containing 20 mg of sample were heated at 5 °C min^{-1} under dry nitrogen and air atmospheres. Scanning electron microscopic (SEM) observations were also carried out to give some indication of the oxide compactness, using a JEOL JSM-6400 instrument.

Crystal Structure Determination of $[SrCu(C_3H_2O_4)_2(H_2O)_4]$. A pale-blue rhombic crystal with the approximate dimensions $0.45 \times 0.20 \times 0.04$ mm was sealed in a capillary and used for data collection on a modified STOE four circle diffractometer. Orientation matrix and lattice parameters were obtained by least-squares refinement of the diffraction data from 34 reflections in the range $15° < 2\theta < 21°$. Data were collected at 298(1) K using graphite crystal-monochromatized Mo Kα radiation ($\lambda = 0.710\,69$ Å) and the ω-scan technique. The intensities were corrected for Lorentz and polarization effects and for absorption.[13] Details on crystal data, intensity collection, and some features of the structure refinement for the compound are reported in Table 1. The structure was solved by direct methods and subsequent Fourier analyses. Anisotropic displacement parameters were applied to the non-hydrogen atoms in full-matrix least-squares refinements. Hydrogen atom positions were obtained from ΔF maps and included in the final refinement cycles by use of geometrical constraints. The programs DIFABS,[13] SHELX-76,[14] SHELXS-86,[15] PLATON,[16] and the X-ray System [17] were used for computations. Analytical expressions of neutral-atom scattering factors were employed, and anomalous dispersion corrections were incorporated.[18] The final atomic positional parameters for the non-hydrogen atoms are listed in Table 2. Selected bond distances and bond angles are given in Table 3.

Table 1. Crystallographic Data for the $[SrCu(C_3H_2O_4)_2(H_2O)_4]$ Compound

molecular formula	$C_6H_{12}O_{12}SrCu$
molecular weight, g mol^{-1}	427.32
space group	*Pccn* (No. 56)
a, Å	6.719(2)
b, Å	18.513(7)
c, Å	9.266(4)
V, Å^3	1152.6(8)
Z	4
T (°C)	25
μ, mm^{-1}	6.40
ρ_{calcd} g cm^{-3}	2.462
ρ_{obsev} g cm^{-3}	2.37(4)
$F_o > 3\sigma(F_o)$	946
$R(F_o)^a =$	0.043
$R_w(F_o^2)^b =$	0.041

^{a} $R(F_o) = [\sum|\Delta F|/\sum|F_o|]$. ^{b} $R_w(F_o^2) = [\sum\{w(\Delta F^2)^2\}/\sum\{w(F_o^2)^2\}]^{1/2}$.

Table 2. Fractional Atomic Coordinates ($\times 10^4$) and Equivalent Isotropic Displacement Parameters (Å^2 $\times$ 10^3) of Non-Hydrogen Atoms for the $[SrCu(C_3H_2O_4)_2(H_2O)_4]$ Compound

atom	*x*	*y*	*z*	U_{eq}[a]
Sr(1)	2500	2500	4688(1)	15(0)
Cu(1)	5000	5000	5000	14(1)
O(1)	5509(7)	4551(2)	3173(4)	18(2)
O(2)	6735(7)	4556(2)	987(5)	18(2)
O(3)	6101(7)	5932(2)	4400(4)	17(2)
O(4)	6607(8)	6792(2)	2843(5)	20(2)
Ow(5)	779(9)	6933(2)	1421(5)	21(2)
Ow(6)	807(8)	6854(3)	4505(5)	23(3)
C(1)	6014(9)	4881(3)	2024(6)	12(3)
C(2)	5633(10)	5683(3)	1871(6)	13(3)
C(3)	6154(10)	6161(3)	3117(6)	13(3)

[a] U_{eq} is defined as one-third of the trace of the orthogonalized $\mathbf{U}_{ij}$ tensor.

Results and Discussion

Description of the Structure. The $[SrCu(mal)_2(H_2O)_4]$ compound can be visualized as a lamellar structure, formed by copper-malonate units, which is infinitely extended along the *a*- and *c*-crystallographic directions (Figure 1). In the unit cell, two nonequivalent water molecules are present, Ow(5) and Ow(6), both of them being coordinated to the strontium ion.

(13) Walker, N.; Stuart, D. *Acta Crystallogr.* **1983**, *A39*, 158.
(14) Sheldrick, G. M. SHELX 76, A Program for Crystal Structure Determination. University Chemical Laboratory: Cambridge, U.K., 1976.
(15) Sheldrick, G. M. SHELX 86. *Acta Crystallogr.* **1990**, *A46*, 467.
(16) Spek, A. L. *Computational Crystallography*; Sayre, D., Ed.; Clarendon Press: Oxford, 1982; p 528.
(17) Stewart, J. M. *The X-ray System*, version of 1976, TR-466. University of Maryland, College Park, 1976.
(18) *International Tables for X-ray Crystallography*; Kynoch: Birmingham, England, 1974; Vol. IV, p 99.

Table 3. Selected Bond Distances (Å) and Angles (deg) for the $[SrCu(C_3H_2O_4)_2(H_2O)_4]$ Compound[a]

Cu(1)−O(1)	1.917(4)	O(1)−C(1)	1.273(7)
Cu(1)−O(3)	1.957(5)	O(2)−C(1)	1.233(7)
Cu(1)−O(2)$_{ii}$	2.515(5)	O(3)−C(3)	1.264(7)
Sr(1)−O(4)$_{i}$	2.705(5)	O(4)−C(3)	1.234(8)
Sr(1)−O(4)$_{ii}$	2.752(5)	C(1)−C(2)	1.513(8)
Sr(1)−Ow(5)$_{viii}$	2.648(6)	C(2)−C(3)	1.496(8)
Sr(1)−Ow(6)$_{iv}$	2.632(5)		

O(4)$_i$−Sr(1)−Ow(5)$_{ix}$	87.2(2)	O(4)$_i$−Sr(1)−Ow(6)$_{iv}$	74.1(2)
O(4)$_i$−Sr(1)−O(4)$_{ii}$	122.6(1)	O(4)$_i$−Sr(1)−O(4)$_{vii}$	154.6(2)
O(4)$_i$−Sr(1)−O(4)$_{vi}$	64.4(1)	O(4)$_i$−Sr(1)−Ow(5)$_{viii}$	134.8(2)
O(4)$_i$−Sr(1)−Ow(6)$_{v}$	78.0(2)	O(4)$_{vii}$−Sr(1)−Ow(5)$_{viii}$	70.3(2)
O(4)$_{vii}$−Sr(1)−Ow(5)$_{ix}$	71.1(1)	O(4)$_{vii}$−Sr(1)−O(4)$_{ii}$	63.2(2)
Ow(6)$_{iv}$−Sr(1)−Ow(5)$_{ix}$	129.3(1)	Ow(5)$_{viii}$−Sr(1)−Ow(5)$_{ix}$	134.4(2)
Ow(6)$_{iv}$−Sr(1)−O(4)$_{ii}$	80.9(2)	Ow(6)$_{iv}$−Sr(1)−O(4)$_{vii}$	130.0(2)
Ow(6)$_{iv}$−Sr(1)−Ow(5)$_{viii}$	65.7(2)	Ow(6)$_{iv}$−Sr(1)−Ow(6)$_{v}$	147.0(2)
O(1)−Cu(1)-O(3)	93.7(2)	O(1)−Cu(1)-O(2)$_{ii}$	88.6(2)
O(2)$_{iii}$−Cu(1)−O(3)	93.5(2)	Cu(1)−O(1)-C(1)	125.3(4)
Cu(1)−O(3)-C(3)	125.0(4)	Cu(1)−O(2)$_{ii}$−C(1)$_{ii}$	117.8(4)
O(1)−C(1)-O(2)	121.4(5)	O(1)−C(1)-C(2)	120.3(5)
C(1)−C(2)-C(3)	117.9(5)	O(3)−C(3)-O(4)	121.3(6)
O(4)−C(3)-C(2)	117.3(5)	O(3)−C(3)-C(2)	121.4(6)

[a] Symmetry codes: (i) $1-x, 1-y, 1-z$, (ii) $-1/2+x, 1-y, 1/2-z$, (iii) $3/2-x, y, 1/2+z$, (iv) $-x, 1-y, 1-z$, (v) $1/2+x, 1/2-y, 1-z$, (vi) $-1/2+x, -1/2+y, 1-z$, (vii) $1-x, -1/2+y, 1/2-z$, (viii) $-x, -1/2+y, 1/2-z$, (ix) $1/2+x, 1-y, 1/2-z$.

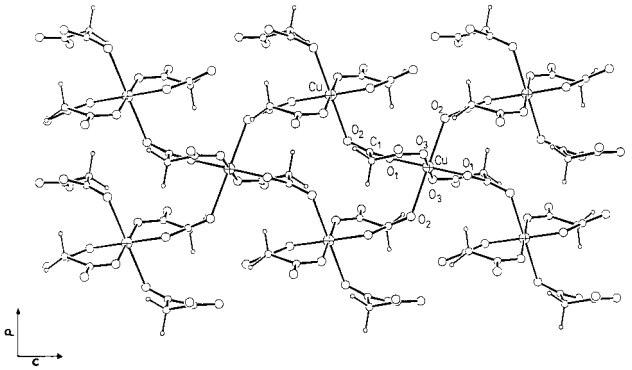

Figure 1. Two-dimensional network of copper polyhedra in $[SrCu(C_3H_2O_4)_2(H_2O)_4]$ (viewed normal to *b*-axis of unit cell).

The copper(II) centers are octahedral, with O(1) and O(3) of two bidentate malonate anions at basal sites (distances of 1.917(4) and 1.957(5) Å, respectively). Coordination is completed via two O(2) atoms at distances of 2.515(5) Å from two other malonate anion molecules at apical sites (Figure 2a). These bridging arrangements by carboxylate groups form infinite sheets in which the closest Cu···Cu separation is 5.72 Å and the exchange distance through the O(2)−C(1)−O(1) atoms is of 6.94 Å. All the bond angles around Cu(1) are close to 90° and similar to those found in related structures.[19] The distortion around the cooper(II) ion has been calculated by quantification of the Muetterties and Guggenberger description.[20,21] The value obtained, $\Delta = 0.2$, is indicative of a regular octahedron with a slight trigonal distortion.

The O(4) atom of the malonate ligand is linked to the strontium ion, forming the three-dimensional network. The strontium ion is also coordinated to four O(4) of different malonate anions, two Ow(5) and two Ow(6) of the lattice water molecules, the average distances being 2.68 Å. In this way,

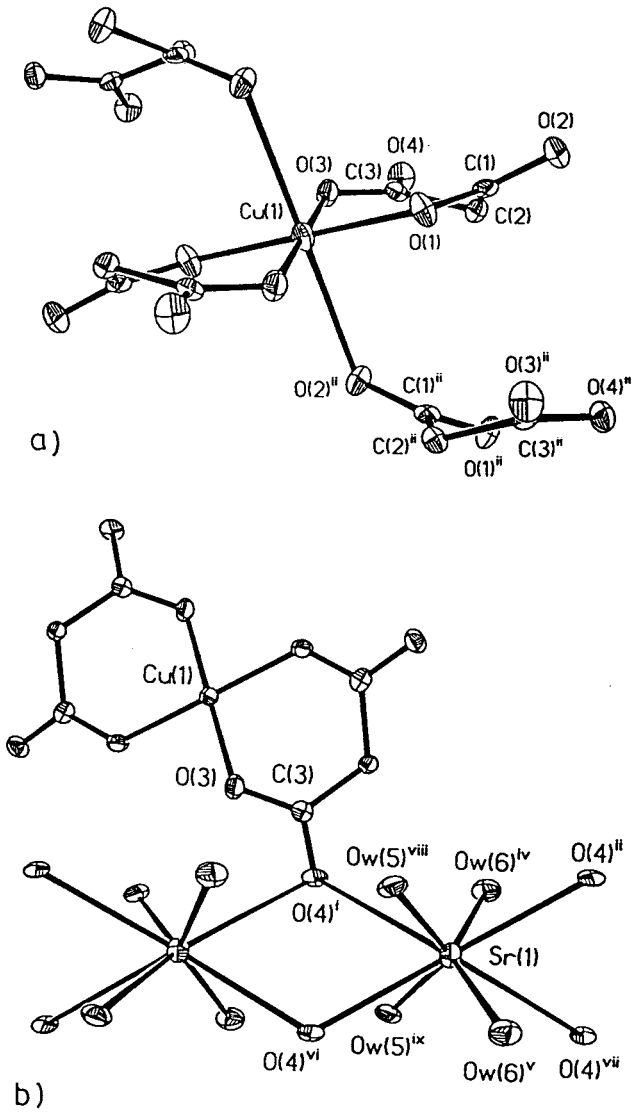

Figure 2. Coordination of (a) copper(II) center and (b) strontium center and junction to copper(II) center in $[SrCu(C_3H_2O_4)_2(H_2O)_4]$.

the coordination polyhedron of the alkaline-earth ion can be visualized as a distorted antiprism (Figure 2b). The crystal structure is stabilized through extensive hydrogen bonding involving the carboxyl groups and water molecules. In this way, copper malonate layers are stacked between strontium cations along the *b* direction, as can be seen in Figure 3. In all the hydrogen bonds, the water oxygens act as donor atoms, and the carboxylate or other water oxygens act as acceptor atoms. The largest acceptor−hydrogen distance is 2.31(8) Å.

In this structure, the malonate ligands have an envelope conformation in which only the methylene group is significantly displaced from the chelate ring plane (Figure 2a). The average C−O distances are 1.25 Å, and the average O−C−O angles are 121°.

In the case of the BaCu, SrMn, and BaMn phases, high-quality crystals were not obtained. X-ray diffraction patterns of the microcrystalline products were performed in the range of $2\theta = 5-70°$, and indexation was made by FULLPROF (pattern matching analysis)[22] on the basis of the orthorhombic cell, space group *Pccn*, and the cell parameters founded for the SrCu phase. The calculated cell parameters are described in

(19) Chattopadhyay, D.; Chattopadhyay, S. K.; Lowe, P. R.; Schwalbe, C. H.; Mazumder, S. K.; Rana, A.; Ghosh, S. *J. Chem. Soc., Dalton Trans.*, **1993**, 913.
(20) Muetterties, E. L.; Guggenberger, L. J. *J. Am. Chem. Soc.* **1974**, *96*, 1748.
(21) Nardelli, M. *Comput Chem.* **1983**, *7*, 95.
(22) Rodriguez-Carvajal, J. *FULLPROF, Program Rietveld Pattern Matching Analysis of Powder Patterns*; Grenoble, IL, nonpublished, 1994.

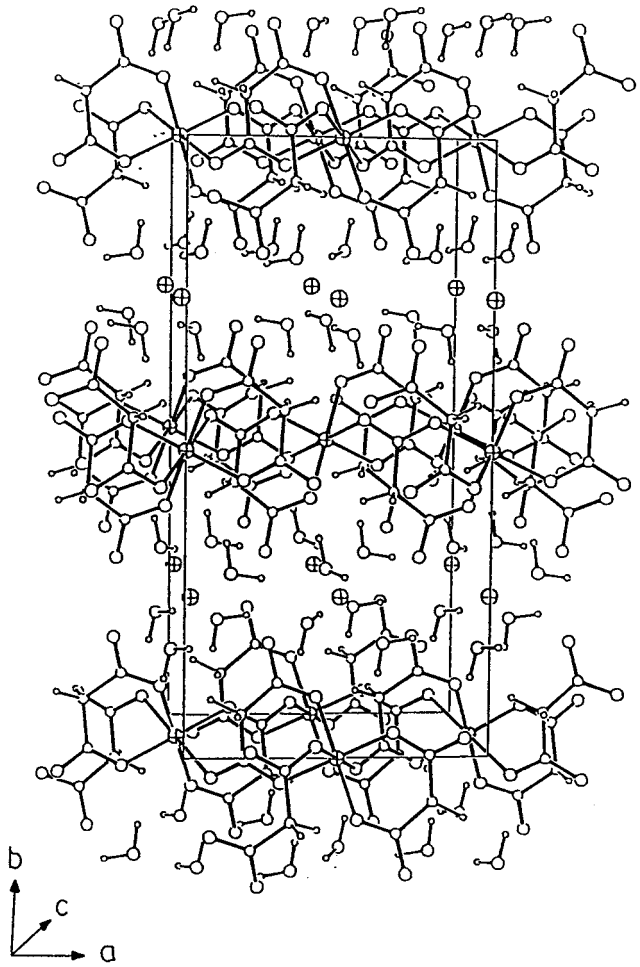

Figure 3. Unit cell plot of the $[SrCu(C_3H_2O_4)_2(H_2O)_4]$ compound.

Table 4. Crystallographic Data for the SrCu, BaCu, SrMn, and BaMn Compounds

compd	$SrCu(L)_2$-$(H_2O)_4$	$BaCu(L)_2$-$(H_2O)_4$	$SrMn(L)_2$-$(H_2O)_4$	$BaMn(L)_2$-$(H_2O)_4$
a (Å)	6.719(2)	6.8703(4)	6.7692(2)	6.8555(5)
b (Å)	18.513(7)	18.9252(6)	18.6160(5)	18.931(1)
c (Å)	9.266(4)	9.4605(6)	9.3932(3)	9.5502(6)
V (Å^3)	1152.6(8)	1230.07(1)	1183.69(3)	1239.4(3)

Table 4. Taking into account these results, we can consider the four phases to be isostructural.

Infrared Spectroscopy. The IR spectra of all compounds are similar. Broad bands are observed in the 3300−3500 cm^{-1} region, which can be assigned to the stretching vibration, υ(O−H), of the hydroxyl groups in the water molecules. The next group of bands appears at around 2900 cm^{-1} and corresponds to the stretching vibration, υ(C−H), of the malonate ligands. The band observed at 1730 cm^{-1} for the malonic acid is shifted in the titled compounds to 1600 cm^{-1}. This fact is indicative of the coordination of all the carboxylate groups to the metal ions. This band appears together with the antisymmetric $\upsilon_a(COO^-)$ vibration. The bands which correspond to the symmetric $\upsilon_s(COO^-)$ vibration are localized in the 1370−1450 cm^{-1} range. Taking into account the relative position of the antisymmetric $\upsilon_a(COO^-)$ and symmetric $\upsilon_s(COO^-)$ vibration bands, we supposed the bonding between the metal and the ligand to be through the formation of a quelate,[23] in good accordance with the crystal data obtained from the SrCu compound. Finally, the bending vibration corresponding to the δ(C═O) group is observed in the 1180−1300 cm^{-1} range, for all compounds

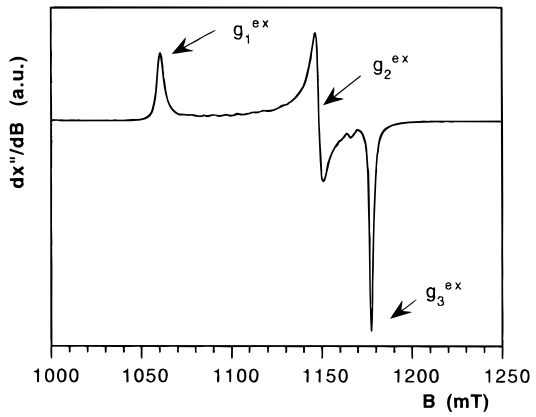

Figure 4. Powder Q-band EPR spectrum of the SrCu compound.

EPR Spectra and Magnetic Properties of the Copper Phases. The Q-band EPR spectra of the $[MCu(mal)_2(H_2O)_4]$ (M = Sr, Ba) compounds are similar. The room-temperature spectrum of the SrCu powdered sample is shown in Figure 4. The EPR measurements of both compounds show an orthorhombic **g** tensor with the following *g*-parameter values: $g_1 = 2.296$, $g_2 = 2.121$, and $g_3 = 2.069$ for SrCu and $g_1 = 2.298$, $g_2 = 2.118$, and $g_3 = 2.071$ for BaCu. The spectra remain unchanged over the temperature range 4.2−298 K. The obtained orthorhombic **g** tensors are not in accordance with the observed axial molecular symmetry. Note that the lowest *g* value 2.07, which is higher than 2.04, suggests the presence of the unpaired electron in the $d_{x^2-y^2}$ orbital,[24] corresponding to an axial symmetry for the copper centers, as was observed from the crystallographic data. Taking into account both the molecular symmetry and the obtained *g* values, we can consider the presence of exchange coupling between two magnetically nonequivalent centers. The exchange interactions between the nearest cooper atoms occur via O(2)−C(1)−O(1) atoms, these copper atoms being symmetrically related by a glide plane along the *ac* plane (see Figure 1). In this way, the EPR spectrum will not show the molecular **g** tensors, but an orthorhombic coupled **g** tensor with g_1^{ex}, g_2^{ex}, and g_3^{ex} values. It will be a linear combination of both molecular symmetry and exchange coupling between the different polyhedra having the canting angle 2α. This angle can be calculated from eq 1, and the obtained value is 51.2° for the SrCu compound, which is in reasonable agreement with the crystallographic 2α (58.5°). For the BaCu compound, the 2α value calculated from eq 1 is 48.9°.

$$\cos 2\alpha = \frac{g_1^{ex} - g_2^{ex}}{g_1^{ex} + g_2^{ex} - 2g_3^{ex}} \qquad (1)$$

Because the $g_\perp$ components of an axial molecular **g** tensor are presumably located in the best equatorial plane,[25] 2α is defined as the canting angle between the normals to the equatorial planes of the two interacting polyhedra and is not necessarily equal to 2α' (crystallographic canting angle between the long axes of the two interacting octahedra).

The resulting molecular **g** tensors calculated by using eq

(23) Nakamoto, K. *Infrared Spectra of Inorganic and Coordination Compounds*, 4th ed.; John Wiley & Sons: New York, 1986.

(24) Hattaway, B. J.; Billing, D. E. *Coord. Chem. Rev.* **1970**, *5*, 143.

(25) Henke, W.; Kremer, S.; Reinen, D. *Inorg. Chem.* **1983**, *22*, 2858.

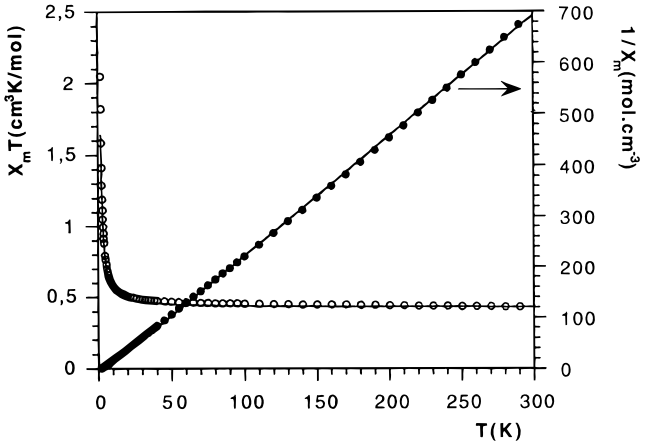

Figure 5. $\chi_M T$ and χ_M^{-1} vs T curves for the SrCu compound.

2−4[26] are $g_{||} = 2.346$, $g_{\perp} = 2.067$ and $g_{||} = 2.337$, $g_{\perp} = 2.071$, for the SrCu and BaCu compounds, respectively.

$$(g_1^{ex})^2 = g_{||}^2 \cos^2 \alpha + g_{\perp}^2 \sin^2 \alpha \quad (2)$$

$$(g_2^{ex})^2 = g_{||}^2 \operatorname{sen}^2 \alpha + g_{\perp}^2 \cos^2 \alpha \quad (3)$$

$$g_3^{ex} = g_{\perp} \quad (4)$$

These results are in good agreement with a $d_{x^2-y^2}$ ground state as was expected from the crystallographic data. Similar results have been observed in other compounds which also present exchange interactions between magnetically different but crystallographically equivalent centers.[27]

The magnetic susceptibility for both compounds was measured from 1.8 to 300 K. The resulting plots of the $\chi_M T$ vs T and $1/\chi_M$ vs T for the SrCu compound are given in Figure 5. The plots of $1/\chi_M$ vs T obey the Curie−Weiss law with positive Weiss constants of $\theta = 3.1$ and 1.8 K and Curie constant (C_m) values of 0.431 and 0.414 cm^3 K mol^{-1} for the SrCu and BaCu compounds, respectively. The C_m experimental values are in good accordance with those obtained from the EPR data. The calculated μ_{eff} values at room temperature are 1.82 and 1.89 μ_B for the strontium and barium compounds, respectively. With decreasing temperature it results in a gradual increase in μ_{eff} value, in good agreement with the presence of ferromagnetic interactions. Taking into account the structural considerations, we fitted the susceptibility data by the expression given by Rushbrooke and Wood for a Heisenberg square-planar system.[28] The expression 5 was deduced by taking into account the $S = {}^1/_2$ value for the Cu(II) ion, based on the spin Hamiltonian $H = -2J\sum_{i,j} S_i S_j$.

$$\chi_M = \frac{Ng^2\beta^2}{4kT}\left[1 - \frac{2}{x} + \frac{2}{x^2} - \frac{1.333}{x^3} + \frac{0.25}{x^4} + \frac{0.4833}{x^5} + \frac{0.003797}{x^6}\right]^{-1} \quad x = \frac{kT}{J} \quad (5)$$

where N is Avogadro's number, β = Bohr magneton, and k = Boltzmann constant.

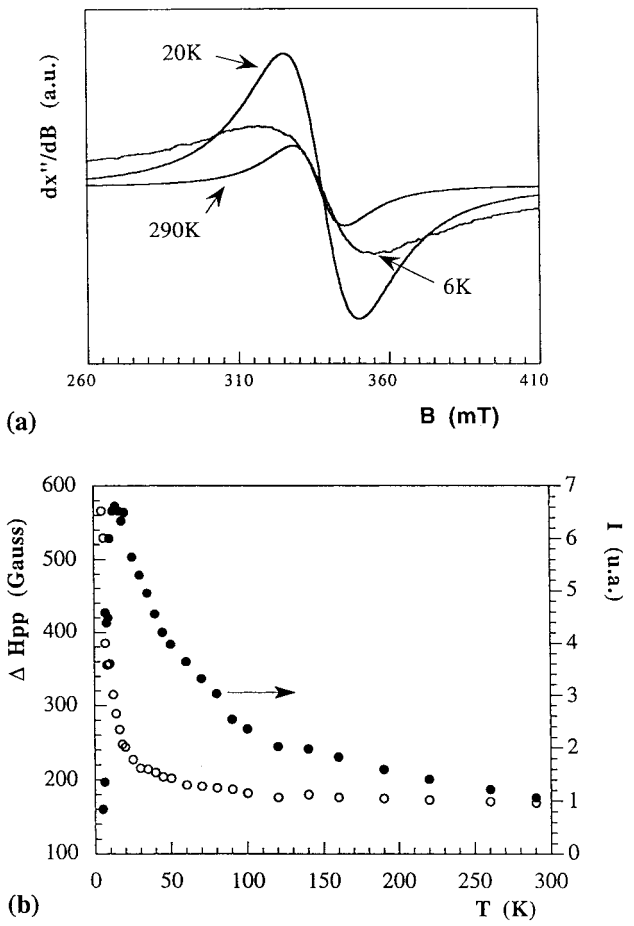

Figure 6. (a) Powder X-band EPR spectra at different temperatures and (b) temperature dependence of the intensity of the signal and the line width curves for the BaMn compound.

The values obtained for the exchange parameters are J/k = 1.44 and 1.15 K with $g = 2.126$ and 2.10 for the strontium and barium compounds, respectively. These g values are in good agreement with those obtained from EPR, $g = 2.16$, for both compounds.

EPR Spectra and Magnetic Properties of the Manganese Phases. The X-band EPR spectra of the $[BaMn(mal)_2(H_2O)_4]$ compound at different temperatures are shown in Figure 6a. Similar results were obtained for the $[SrMn(mal)_2(H_2O)_4]$ compound. Both of them show isotropic signals centered around $g = 2$ in all of the temperature ranges studied. The temperature dependence of the intensity of the signal and the line width for the BaMn compound are shown in Figure 6b. The intensity of the signal calculated by integration over the magnetic field range 2400−4200 G increases up to 20 K, in the range where the curve follows the Curie−Weiss law, and then decreases, not being detectable below 7 K. The line width increases slightly with temperature up to approximately 20 K, where it increases vigorously. The increase, at low temperatures, compensates for the decreasing intensity of the signal. These results are in good agreement with those observed for other 2D antiferromagnets, where it has been observed that the line width increases dramatically when the temperature reaches the T_{Neel} point.[29−30] In the titled compounds, the value of the line width is around

(26) Calvo, R.; Mesa, M. A. *Phys. Rev. B* **1983**, *28*, 1244.
(27) (a) Levstein, P. R.; Calvo, R.; Castellano, E. E.; Piro, O. E.; Rivero, B. E. *Inorg. Chem.* **1990**, *29*, 3918. (b) Rojo, T.; Insausti, M.; Lezama, L.; Pizarro, J. L.; Arriortua, M. I.; Calvo, R. *J. Chem. Soc., Faraday Trans.* **1995**, *91*, 423.
(28) Rushbrooke, G. S.; Wood, P. *J. Mol. Phys.* **1963**, *6*, 409.
(29) (a) Wijn, H. W.; Walker, L. R.; Daris, J. L.; Guggenheim, H. *J. Solid State Commun.* **1972**, *11*, 803; (b) Richards, P. M.; Salamon, M. B. *Phys. Rev. B* **1974**, *9*, 32.
(30) Escuer, A.; Vicente, R.; Goher, M. A. S.; Mautner, F. A. *Inorg. Chem.* **1995**, *34*, 5707.

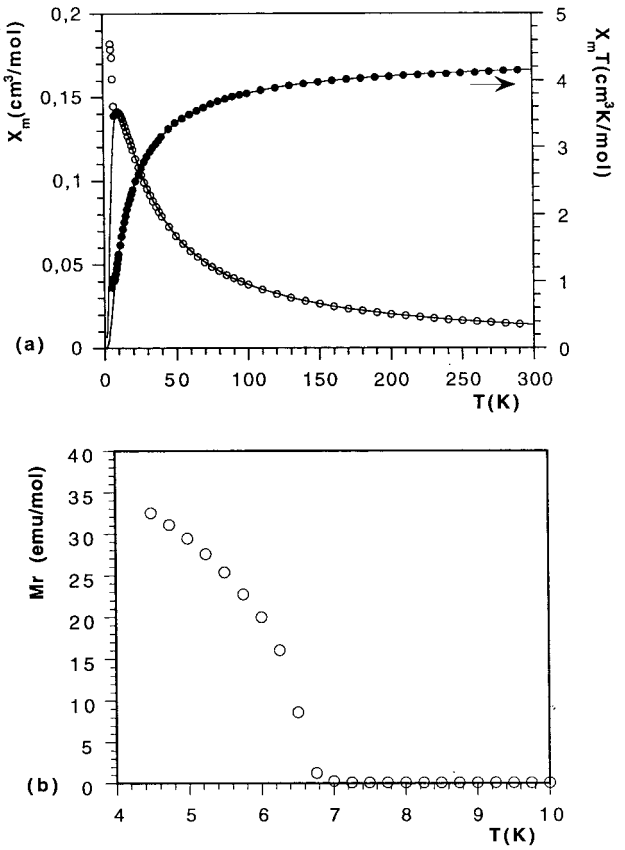

Figure 7. (a) $\chi_M T$ and χ_M vs T curves and (b) zero field magnetization vs T curve for the BaMn compound cooled under a magnetic field of 100 Oe.

566 G at 5 K, which is lower than those found for other 2D antiferromagnets.[29] However, this fact is in accordance with the weak antiferromagnetic interaction observed in our compounds due to the large Mn···Mn separation, through the O−C−O atoms.[31] At higher temperatures, the line width increases very slowly, probably due to the weak character of the antiferromagnetic interactions appearing in the compound.

Variable-temperature magnetic susceptibility measurements were performed on powdered samples in the 1.8−300 K range. The plots of $\chi_M T$ and χ_M vs T for the BaMn compound are given in Figure 7a. The susceptibility increases with decreasing temperature, reaching a value of $T_{max} = 10$ K, and then decreases until 7.5 K and at lower temperatures increases again. Similar curves showing a maximum at 12 K and a minimum at 8.5 K were observed for the SrMn compound. The μ_{eff} values are 6.07 and 6.04 μ_B at room temperature, for the SrMn and BaMn compounds, respectively, which are close to the spin-only value for the Mn(II) ion. The decrease of the $\chi_M T$ until around 7 K is indicative of a small antiferromagnetic interaction, and considering the structural features, this behavior can be considered as a 2D Heisenberg antiferromagnet. In this way, the high-temperature susceptibility data have been fitted to the expansion series (eq 6) given by Rushbrooke and Wood,[28]

$$\chi_M = 2.91 \frac{Ng^2\beta^2}{kT}[1 + 23.33x + 147.78x^2 + 405.48x^3 + 8171.3x^4 + 64968x^5 + 15811x^6]^{-1} \quad (6)$$

where $x = J/kT$.

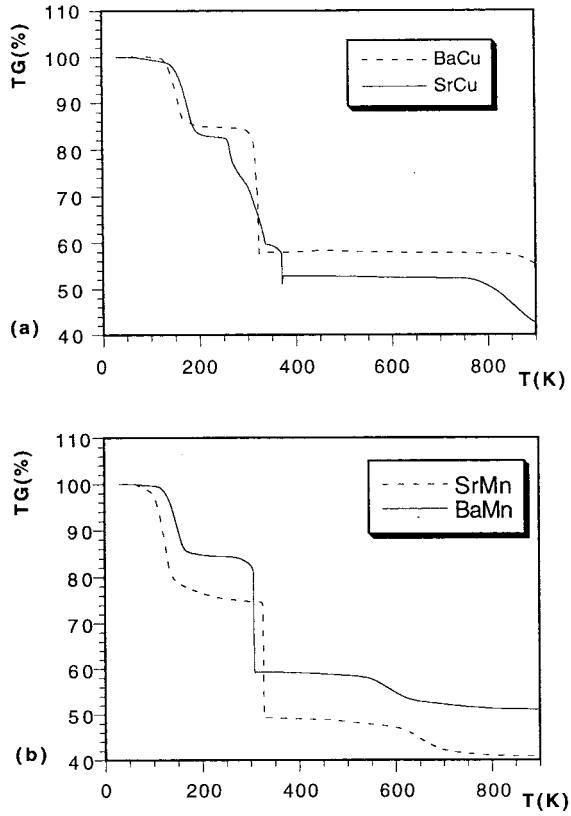

Figure 8. *TG* curves of $[MM'(C_3H_2O_4)_2(H_2O)_4]$ compounds (a) M = Sr, Ba; M′ = Cu and (b) M = Sr, Ba; M′ = Mn, in air atmosphere.

All of the other symbols have the usual meaning for an $S = {}^5/_2$ antiferromagnetic layer. The best fit parameters are $g = 2.00$ and $J/k = -0.65$ K for SrMn and $g = 1.993$ and $J/k = -0.587$ K for the BaMn compound, which lead to the theoretical curve represented as a solid line in Figure 7a. So, up to temperatures of 7 K these compounds show a 2D Heisenberg antiferromagnet behavior with a weak intralayer antiferromagnetic interaction between the Mn(II)···Mn(II) atoms through the O−C−O bridges. However, the presence of a minimum in the $\chi_M T$ curve at 5 K together with a sudden increase suggests that the total alignment of the spins is not produced at low temperatures. The high spin of Mn(II), compared with that of Cu(II), implies that more magnetic orbitals take part in the different exchange pathways and more interactions could be competing between them. Such behavior is typical of the 1D and 2D antiferromagnetic systems showing a weak ferromagnetism at low temperature (canting).[32] The existence of a maximum in the $\chi_M T$ curve at lower temperatures could be indicative of the presence of long-range magnetic ordering due to antiferromagnetic couplings between layers below 1.8 K. To confirm the existence of weak ferromagnetism and to calculate the Neel temperature, zero field magnetization measurements with temperature were carried out for the BaMn compound after cooling it down under a magnetic field of 100 Oe. The results are shown in Figure 7b. As can be seen, below $T_{Neel} = 7$ K, the FCM curve shows a rapid increase without reaching saturation. This fact indicates the presence of weak ferromagnetism intralayer.

Thermal Analysis. The decomposition steps of the compounds were obtained from their *TG* curves (Figure 8), which show the occurrence of three consecutive processes, namely,

(31) Tangoulis, V.; Psomas, G.; Dendrinou-Samara, C.; Raptopoupou, C. P.; Terzis, A.; Kessissoglou, D. P. *Inorg. Chem.* **1996**, *35*, 7655.

(32) Carlin, R. L. *Magnetochemistry*; Springer-Verlag: Berlin, 1986; pp 206−212.

dehydration, ligand pyrolysis, and inorganic residue formation. No significant differences between the treatments in air and nitrogen atmospheres were observed, but only slight displacements in the decomposition temperature ranges were seen. The first process occurs in the range 100−200 °C and corresponds to the loss of the four water molecules present in these compounds. This process seems to take place in only one step, suggesting that all of the water molecules are similar, as was deduced from the crystallographic data for the SrCu compound. The following stage, which occurs in the temperature range 260−350 °C, involves decarboxylation of the ligand. The most reasonable reaction schemes to describe the decomposition proccess are the following:

$$MM'L_2(s) \rightarrow MCO_3(s) + M'CO_3(s) + R(g) \qquad (a)$$

$$MM'L_2(s) \rightarrow MO(s) + M'CO_3(s) + R(g) \qquad (b)$$

$$MM'L_2(s) \rightarrow MO(s) + M'O(s) + R(g) \qquad (c)$$

In the control of these pyrolysis results, the nature of the cation coordinated to the ligand may be the main factor.[33] Depending on the stability of the metal carbonates, a, b, or c reactions can occur. In our case, as alkaline-earth metal carbonates are stable, the ligand pyrolysis can be described by the second reaction. The weight loss is in good accordance with the formation of the alkaline-earth carboxylate and the transition metal oxide. This step remains stable until carbonates decompose to react with oxides and yield mixed oxides.

Evolution of the Inorganic Residue. Taking into account the previous analysis, we performed thermal treatments in tubular furnaces in air atmosphere, with the aim of obtaining pure phases of mixed oxides. In this sense, the malonate precursors were fired at 400 °C for 12 h to remove the organic part, followed by treatments at higher temperatures. The resulting products were characterized by X-ray powder diffraction (see Figure 9).

In the case of the copper(II) compounds, the $MCuO_2$ (M = Sr, Ba) mixed oxides were obtained after firing the precursors at 800 °C. At lower temperatures, mixtures of copper(II) oxide and alkaline-earth metal carbonates were observed, according to the b reaction of the previous decomposition scheme. For the strontium−copper system, the CuO and $SrCO_3$ compounds were present in the inorganic up to until 600 °C. The Cu_2SrO_3 oxide was detected together with $SrCO_3$ at 700 °C, and finally, the $SrCuO_2$ phase[34] was obtained as pure phase after a thermal treatment of 800 °C for 3 h. This phase was indexed with the space group *Cmcm* and the unit cell parameters $a = 3.575(1)$, $b = 16.370(7)$, and $c = 3.915(1)$ Å. Its structure can be described as an intergrowth of simple rock salt layers and an oxygen deficient ReO_3-type shear structure.[35] For the barium compound, the mixture of the CuO and $BaCO_3$ phases was observed up to 700 °C. After a thermal treatment at 800 °C for 10 h, the $BaCuO_2$ oxide appears as pure phase.[36,37] The longer thermal treatment with respect to the strontium phase is probably due to the increasing stability of the carbonate down

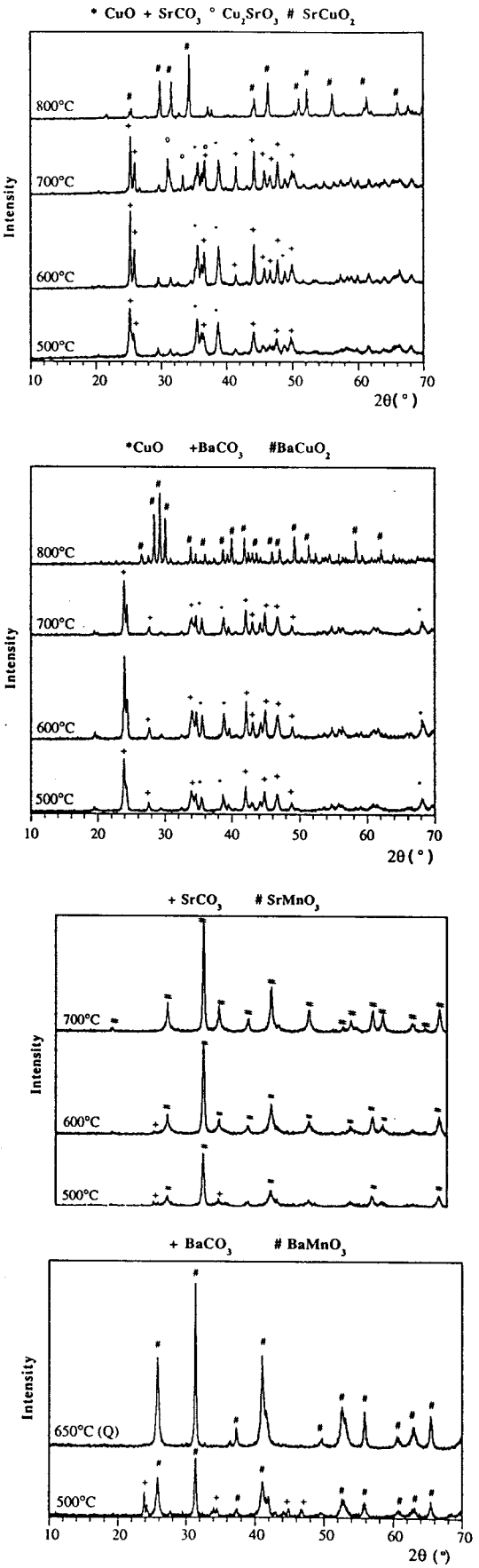

Figure 9. X-ray diffraction diagrams of the phases obtained at different temperatures from the (a) $[SrCu(C_3H_2O_4)_2(H_2O)_4]$, (b) $[BaCu(C_3H_2O_4)_2(H_2O)_4]$, (c) $[SrMn(CH_3H_2O_4)_2(H_2O)_4]$, and (d) $[BaMn(CH_3H_2O_4)_2(H_2O)_4]$ compounds.

(33) Escrivá, E.; Fuertes, A.; Folgado, J. V.; Marinez-Tamayo, E.; Beltrán-Porter, A.; Beltrán-Porter, D. *Thermochim. Acta* **1986**, 104, 223.
(34) Powder Diffraction File, Card No. 38-1179. Joint Committe on Powder Diffraction Standards, Swarthmore, PA, 1984.
(35) Teske, C. L.; Müller-Buschbaum, H. K. *Z. Anorg. Allg. Chem.* **1970**, *379*, 234.
(36) Powder Diffraction File, Card No. 38-1402. Joint Committe on Powder Diffraction Standards, Swarthmore, PA, 1984.
(37) Paulus, E. F.; Miehe, G.; Fuess, H.; Yehia, I.; Löchner, V. *J. Solid State Chem.* **1991**, *90*, 17.

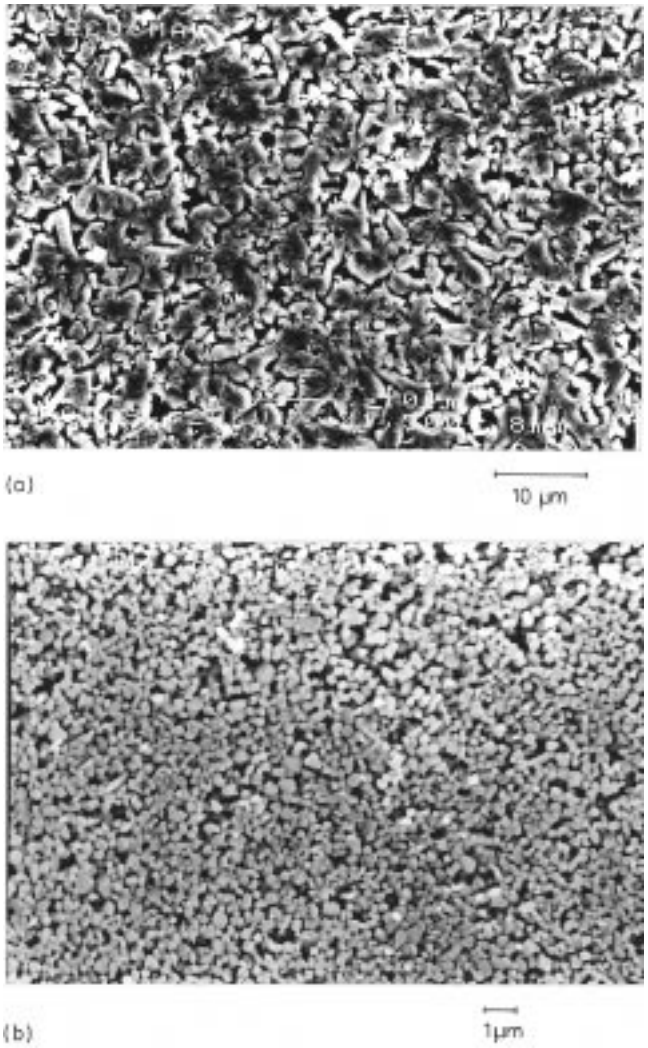

Figure 10. SEM photographs of the (a) $SrCuO_2$ compound obtained at 800 °C and (b) $BaMnO_3$ compound obtained at 650 °C.

the group. The obtained oxide, $BaCuO_2$, was indexed on the basis of the space group *Im*3*m*, given in ref 37 and of the unit cell parameter $a = 18.272(1)$ Å. Recently, the tendency of this oxide to introduce carbonate in the structure has been observed.[38] To detect the presence of carbonates in the final oxide, IR experiments were performed. The IR spectrum shows bands at 1400 and 856 cm^{-1} which can be attributed to the presence of oxocarbonates, which would be occuping the disordered region of the structure.[38] Note that the attainment of these copper compounds using the traditional ceramic method requires higher reaction temperatures and times. In this sense, temperatures of 900 °C and lengths of time 2 or 3 times longer than those employed with the metallo-organic method are necessary.[39−40]

The manganese oxides were obtained at lower temperatures than the homologous ones of copper(II). In this way, the presence of the $MMnO_3$ (M = Sr, Ba) phase was already observed at 500 °C as the majority phase, but some carbonate residues were also present. For the strontium compound, temperatures of 700 °C were necessary in order to eliminate all the carbonate and to get the $SrMnO_3$ oxide as the pure phase.[41] This oxide was indexed with the space group $P6_3/mmc$ and the unit cell parameters $a = 5.448(2)$ and $c = 9.073(4)$ Å. For the barium manganese compound, mixtures of $Ba_3Mn_2O_8$ and $BaMnO_3$ oxides were found in the residue obtained after several thermal treatments for both reactions at higher temperatures (700 °C for 10 h) and longer reaction times (20 h at 600 °C). To avoid the formation of the $Ba_3Mn_2O_8$ phase, the inorganic residue was quenched at 650 °C, and the $BaMnO_3$ oxide was obtained as the pure phase.[42] This final oxide was indexed with the space group $P6_3/mmc$ and the unit cell parameters $a = 5.469(4)$ and $c = 4.811(5)$ Å. It is interesting to note that by using the ceramic method, temperatures of 1000 °C and reaction times of two weeks were needed to obtain the same manganese phases.[43]

Scanning Electron Microscopy. Scanning electron microscopic photographs of the $SrCuO_2$ and $BaMnO_3$ oxides pellets are shown in Figure 10. Similar morphologies have been obtained for the $BaCuO_2$ and $SrMnO_3$ oxides. As can be seen for the $MCuO_2$ oxides, uniform small particles of approximately $1 \times 2\ \mu m^2$ were obtained. In some cases, the small size of the particles leads to a preliminary sintering process, as noted by the formation of small "necks" between the particles. On the other hand, for the M−Mn−O system, submicroparticles have been obtained, this grain size being the best morphology for a further sinterization. The smaller grain size observed in the manganese phases, in relation to that obtained for the copper phases, can be related to the lower reaction temperatures used in the attainment of theses oxides. This fact is characteristic of the soft process of decomposition from the metallo-organic precursors.

Concluding Remarks

The $[MM'(C_3H_2O_4)_2(H_2O)_4]$ (M = Ba, Sr and M′ = Cu, Mn) compounds crystallize in the *Pccn* space group with similar cell dimensions. Taking into account the crystallographic data obtained from the SrCu structure, we could visualize all the compounds as lamellar phases, formed by copper−malonate or manganese−malonate units, which are infinitely extended along the *ac* direction. In this way, 2D ferromagnetic and antiferromagnetic interactions were observed for the copper and manganese compounds, respectively, the susceptibility data being fitted by the expression corresponding to a Heisenberg square-planar system. An exchange coupling between magnetically different but crystallographically equivalent molecular **g** tensors has been observed from the EPR spectra of the copper phases. For the manganese compounds, at temperatures below $T_{Neel} = 7$ K, the total coupling of the antiparallel spins is not produced. This magnetic ordering can be interpreted due to the presence of weak ferromagnetism. The spin for Mn(II) being higher than for Cu(II) implies that more magnetic orbitals are present in the different exchange pathways and therefore, more interactions could be competing between them. EPR measurements for these compounds are in good accordance with the magnetic ones. It is supposed that the greater the spin coupling, the greater the intensity of the EPR line and the line width. However, at

(38) (a) Aranda, A. G.; Attfield, J. P. *Angew. Chem., Int. Ed. Engl.* **1993**, *32*, 1454. (b) Insausti, M.; Lezama, L.; Cortés, R.; Gil de Muro, I.; Rojo, T.; Arriortua, M. I. *Solid State Commun.* **1995**, *93*, 823.
(39) Hwang, N. M.; Roth, R. S.; Rawn, C. J. *J. Am. Ceram. Soc.* **1990**, *73*, 2531.
(40) (a) Hodorowicz, S. A.; Lasocha, W.; Lasocha, A.; Eick, H. A. *J. Solid State Chem.* **1988** *77*, 148. (b) Jones, R.; Janes, R.; Armstrong, R.; Pyper, N. C.; Edwards, P. P.; Keeble, D. J.; Harrison, M. R. *J. Chem. Soc., Faraday Trans.* **1990**, *86*, 675.
(41) Powder Diffraction File, Card No. 24-1213. Joint Committe on Powder Diffraction Standards, Swarthmore, PA, 1984.
(42) Powder Diffraction File, Card No. 26-168. Joint Committe on Powder Diffraction Standards, Swarthmore, PA, 1984.
(43) Negas, T.; Roth, R. S. *J. Solid State Chem.* **1970**, *1*, 323; Negas, T.; Roth, R. S. *J. Solid State Chem.* **1971**, *3*, 323.

temperatures below 10 K, the intensity of the line decreases considerably. This decrease can be compensated for with the high increase of the line width at those temperatures. It can be also deduced that in all cases, the oxides obtained from the metallo-organic precursors have been prepared at relatively short times and low temperatures, compared with the ceramic method. In this sense, in the case of the manganese systems, temperatures of 650 °C and reaction times of 10 h were needed. Finally, the usefulness of soft chemical routes in order to obtain homogeneous and small particles has been shown. Taking into account the fact that all the compounds are isostructural, we have prepared several solid solutions with the formula $[MM'_{1-x}M''_x(C_3H_2O_4)_2(H_2O)_4]$ (M′, M″ = transition metal and M = alkaline-earth metal) with the aim of obtaining the $MM'_{1-x}M''_xO_{3-x}$ oxides after the corresponding thermal treatments. Preliminary experiments display good results which, together with the magnetic properties, will be published shortly.

Acknowledgment. This work has been carried out with the financial support of the Ministerio de Educación y Ciencia (DGICYT PB94-0469 grant) which we gratefully acknowledge. F.A.M. thanks Prof. Kratky for the use of experimental equipment. I.G.M. wishes to thank the Spanish "Ministerio de Educación y Ciencia" for a doctoral fellowship.

Supporting Information Available: Listings of structural determinations, anisotropic displacement parameters, bond distances and angles, torsion angles, molar magnetic susceptibility vs temperature data (3 pages). Ordering information is given on any current masthead page.

IC9800132